

## Saur Vidyut Kosh IV: STUDY OF A RECHARGEABLE SOLAR BATTERY WITH $n\text{-Pb}_3\text{O}_4$ ELECTRODES

MAHESHWAR SHARON, SUDHIR KUMAR and N. P. SATHE

*Department of Chemistry, Indian Institute of Technology, Bombay 76 (India)*

S. R. JAWALEKAR

*Department of Electrical Engineering, Indian Institute of Technology, Bombay 76 (India)*

(Received September 21, 1983; accepted February 13, 1984)

### Summary

The semiconductor  $n\text{-Pb}_3\text{O}_4$  ( $E_g = 2.1$  eV) was prepared by the citrate method, and the conversion efficiency of the photoelectrochemical cell  $n\text{-Pb}_3\text{O}_4|\text{Fe}^{3+}, \text{Fe}^{2+}|\text{Pt}$  was found to be 0.09%. A Saur Vidyut Kosh (rechargeable solar battery) of the following type was then prepared:

$n\text{-Pb}_3\text{O}_4, \text{Pt}|\text{Fe}^{3+} (10^{-1} \text{ M}), \text{Fe}^{2+} (\text{saturated})||\text{IO}_3^- (10^{-1} \text{ M}), \text{I}^- (10^{-1} \text{ M})|\text{Pt}$

The dark potential of the charged battery was 0.84 V; the charging efficiency of the battery was 72%. The energy diagram of  $n\text{-Pb}_3\text{O}_4$  calculated from the experimentally determined flat-band potential  $V_{fb}$  ( $-0.31$  V measured with respect to a standard calomel electrode) was found to differ from the values calculated by the Butler-Ginley method. The  $\text{Pb}_3\text{O}_4$  electrode appears to corrode photoelectrochemically. However, when a saturated solution of  $\text{Fe}^{2+}$  was used, the rate of corrosion appeared to slow down.

### 1. Introduction

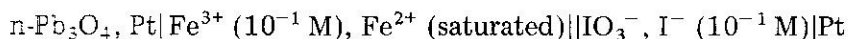
Research into the development of a photoelectrochemical solar cell, utilizing a stable photoanode and photocathode, is not a new idea [1 - 4]. However, like photovoltaic cells, the photoelectrochemical cell does not have the capability to store energy. Therefore efforts have been made [5, 6] to prepare a rechargeable solar battery (a Saur Vidyut Kosh) which can store energy.

In such a battery, unlike photoelectrochemical cells, the cathodic and anodic chambers are separated by a membrane [4, 7 - 9]. The two half-cells contain two different redox systems.

Since  $\text{PbO}_2$  is the most common acid-resistant electrode in lead-acid batteries and since not much work has been reported on the various oxides of lead, we launched studies on  $\text{Pb}_3\text{O}_4$ ,  $\alpha\text{-PbO}$  and  $\beta\text{-PbO}_2$  ( $E_g = 2.1$  eV,

1.8 eV and 1.6 eV respectively) to determine their suitability for use as photoelectrodes in photoelectrochemical cells.

In the work reported in the present paper, n-Pb<sub>3</sub>O<sub>4</sub> electrodes were prepared and characterized photoelectrochemically. A Saur Vidyut Kosh (rechargeable solar battery) of the following type was then designed and fabricated:



## 2. Experiments and results

AnalaR grade chemicals were used in all the experiments without any further purification. The intensity of light at the electrodes was maintained at 60 mW cm<sup>-2</sup> with the help of a quartz-halogen lamp (225 W).

### 2.1. Preparation of the electrodes

Orange-red Pb<sub>3</sub>O<sub>4</sub> powder was prepared by the thermal decomposition of lead citrate (prepared from 99.99% pure lead) at 350 °C in an oxygen atmosphere for 2 h. The Pb<sub>3</sub>O<sub>4</sub> was identified by X-ray diffraction studies.

Pellets of Pb<sub>3</sub>O<sub>4</sub> (thickness, 2 mm; diameter, 1 cm) showed a high resistivity (10<sup>12</sup> Ω cm) after being sintered in air at 350 °C for 2 h. The resistivity was decreased by reducing the pellet in a hydrogen atmosphere at various temperatures. The photoresponse of each pellet was then measured using the cell n-Pb<sub>3</sub>O<sub>4</sub>|H<sub>2</sub>SO<sub>4</sub>|Pt (Table 1). Silver paste was used as an ohmic contact.

TABLE 1

<i>Pellet</i>	<i>Temperature</i> (°C)	<i>Time</i> (h)	<i>Resistivity</i> (Ω cm)	<i>J<sub>ph sc</sub></i> (μA cm <sup>-2</sup> )	<i>V<sub>ph oc</sub></i> (V)
1	200	2	10 <sup>5</sup>	50	0.06
2	250	2	10 <sup>4</sup>	60	0.12
3	300	2	0.5	100	0.26
4	350	2	2	30	0.03
5	400	2	3	23	0.02

From the results shown in Table 1, it is obvious that the pellets sintered at 300 °C for 2 h gave the best photoresponse. Pellets made under these conditions were therefore used in all subsequent work. However, many of the pellets prepared under identical conditions did not give reproducible photoresponses.

## 2.2. Photoelectrochemical characterization

### 2.2.1. Selection of the redox couple

To fabricate a photoelectrochemical solar cell a suitable redox couple with (a) an appropriate redox potential and (b) optimum concentration is required. The conduction band edge has been calculated [10] to be 4.79 eV (or 0.29 V measured with respect to a standard hydrogen electrode (SHE)) and the valence band edge to be 6.97 eV (or 2.47 V (SHE)). Accordingly, we chose to study the photoresponse of redox couples with  $E_{\text{redox}}^{\circ}$  between 0.29 and 2.47 V, e.g.  $\text{I}_2|\text{I}^-$  (0.53 V),  $\text{Fe}^{3+}|\text{Fe}^{2+}$  (0.77 V),  $\text{Cr}^{6+}|\text{Cr}^{3+}$  (1.10 V) and  $\text{Ce}^{4+}|\text{Ce}^{3+}$  (1.45 V).

The photoresponse of the n-Pb<sub>3</sub>O<sub>4</sub> electrode was measured with each of the above-mentioned electrolytes (pH 1; 0.1 M) using platinum as the counterelectrode. It was found that the  $\text{Fe}^{3+}|\text{Fe}^{2+}$  redox couple gave the maximum photoresponse and hence this was selected as the most suitable electrolyte for this cell. However, it was necessary to determine the best combination of concentrations of  $\text{Fe}^{3+}$  and  $\text{Fe}^{2+}$  ions. For this purpose a set of experiments was carried out; the results are shown in Table 2.

TABLE 2

	$\{[\text{Fe}^{3+}] (\text{M})\}/\{[\text{Fe}^{2+}] (\text{M})\}$	Ratio	Photocurrent density ( $\mu\text{A cm}^{-2}$ )
a	$10^{-6}/10^{-1}$	$10^{-5}$	63.80
b	$10^{-5}/10^{-1}$	$10^{-4}$	66.40
c	$10^{-4}/10^{-1}$	$10^{-3}$	68.10
d	$10^{-3}/10^{-1}$	$10^{-2}$	102.6
e	$10^{-2}/10^{-1}$	$10^{-1}$	106.1
f	$10^{-1}/10^{-1}$	1	137.1
g	$1/10^{-1}$	10	137.1
h	Saturated/ $10^{-1}$	—	115.1
i	$10^{-1}/1$	$10^{-1}$	115.9
j	$10^{-1}$ /saturated	—	175.2
k	Saturated/saturated	1	75.2

These experiments suggest that the concentrations  $\text{Fe}^{3+}$  ( $10^{-1}$  M) and  $\text{Fe}^{2+}$  (saturated) gave the highest photoresponse.

### 2.2.2. Band gap measurement

The band gap was determined first by a reflectance measurement technique [11]. The wavelength corresponding to a maximum in the plot of  $dT/d\lambda$  versus  $\lambda$  gave a band gap of 2.1 eV (Fig. 1) where  $T$  is the transmittance and  $\lambda$  is the wavelength of the light.

In a second method using the photoelectrochemical cell n-Pb<sub>3</sub>O<sub>4</sub>| $\text{Fe}^{3+}$ ,  $\text{Fe}^{2+}$ |Pt the photocurrent density was measured by illuminating the electrode through a monochromator for different wavelengths. The quantity  $(J_{\text{ph}}/h\nu)^2$  where  $J_{\text{ph}}$  is the photocurrent density was plotted against wave-

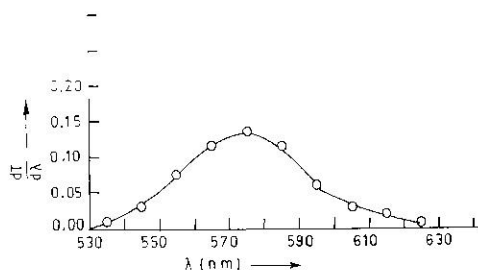


Fig. 1. Differential reflectance spectra of  $\text{Pb}_3\text{O}_4$  powder ( $\lambda_{\text{max}} = 575 \text{ nm}$ ).

length. The intercept of the linear plot [12, 13] with the  $h\nu$  axis gave a value for the band gap of 2.0 eV. The band gaps determined by these methods are in agreement with the reported value (2.18 eV) [14].

### 2.2.3. Flat-band potential measurement

Using the same photoelectrochemical cell, the flat-band potential of the semiconductor electrode was measured by plotting  $I_{\text{ph}}^2$  versus  $V$  (the biasing potential) [12]. The intercept of the linear plot with the axis of potential gave the value of the flat-band potential of the electrode ( $-0.31 \text{ V}$  measured with respect to a standard calomel electrode (SCE)).

### 2.2.4. Power efficiency and fill factor

The maximum power efficiency and the fill factor were calculated from the  $I$ - $V$  characteristics of the photoelectrochemical cell (Fig. 2). The photocurrent and photovoltage of the semiconductor electrode were measured at different biased potentials. The fill factor and power efficiency were calculated to be 0.38 and 0.09% respectively. The low power efficiency is not unreasonable because of the high band gap of the semiconductor.

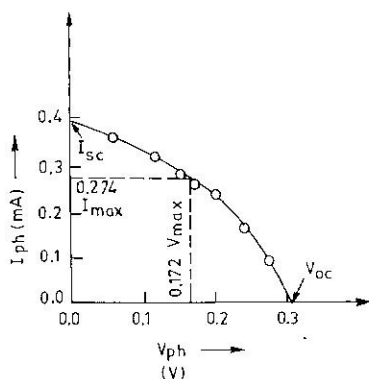


Fig. 2.  $I$ - $V$  characteristics of a  $\text{Pb}_3\text{O}_4$  photoanode showing  $I_{\text{max}}$  and  $V_{\text{max}}$ .

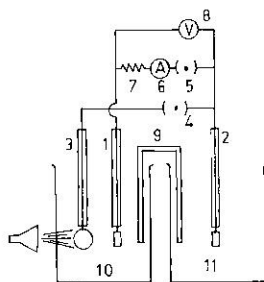


Fig. 3. A schematic diagram of a Saur Vidyut Kosh: 1, 2, platinum electrodes; 3,  $\text{Pb}_3\text{O}_4$  electrode; 4, 5, keys; 6, milliammeter; 7,  $100 \Omega$  resistor; 8, millivoltmeter; 9, salt bridge; 10, compartment 1 containing  $\text{Fe}^{3+}/\text{Fe}^{2+}$ ; 11, compartment 2 containing  $\text{IO}_3^-/\text{I}^-$ .

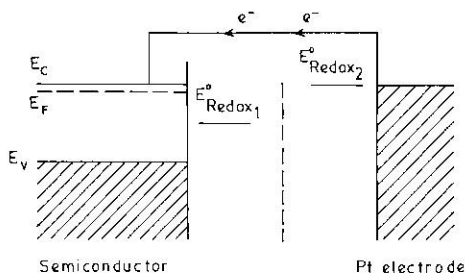


Fig. 4. Relative positions of  $E^{\circ}_{\text{redox}}$  in the two compartments of a Saur Vidyut Kosh.

### 2.3. Saur Vidyut Kosh

The above-mentioned photoelectrochemical cell was used for preparing a rechargeable solar battery (Fig. 3). The battery was charged by short circuiting the n-Pb<sub>3</sub>O<sub>4</sub> electrode 3 and the platinum electrode 2; discharging took place between the two platinum electrodes. In the charging and discharging processes, key 4 and key 5 respectively were kept open. The momentary discharge current was measured through a 100  $\Omega$  resistor at intervals of 10 min. The choice of the electrolyte Fe<sup>3+</sup>|Fe<sup>2+</sup> in compartment 1 had already been decided on the basis of obtaining the maximum photocurrent. In order to facilitate the discharging process in the dark,  $E^{\circ}_{\text{redox}}$  of the electrolyte in compartment 2 should be more negative (with respect to an SHE) than that in compartment 1 (Fig. 4). With this in mind, we tried four redox couples I<sub>2</sub>|I<sup>-</sup>, Fe(CN)<sub>6</sub><sup>3-</sup>|Fe(CN)<sub>6</sub><sup>4-</sup>, IO<sub>3</sub><sup>-</sup>|I<sup>-</sup> and Cu<sup>2+</sup>|Cu to determine which was the best to use. The current density and voltage output were measured for each of the redox couples (Table 3) and the IO<sub>3</sub><sup>-</sup>|I<sup>-</sup> redox system was found to be the most suitable electrolyte for compartment 2. Therefore, the final structure of the rechargeable solar battery was

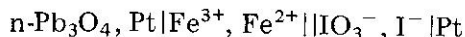


TABLE 3

Redox couple compartment 1	Redox couple compartment 2	pH	$J$ ( $\mu\text{A cm}^{-2}$ )	$V$ (mV)	Time of charging (min)
Fe <sup>3+</sup>  Fe <sup>2+</sup>	I <sub>2</sub>  I <sup>-</sup>	4	50	26	60
Fe <sup>3+</sup>  Fe <sup>2+</sup>	Fe(CN) <sub>6</sub> <sup>3-</sup>  Fe(CN) <sub>6</sub> <sup>4-</sup>	9	158.5	29	60
Fe <sup>3+</sup>  Fe <sup>2+</sup>	IO <sub>3</sub> <sup>-</sup>  I <sup>-</sup>	8	408.0	93	60
Fe <sup>3+</sup>  Fe <sup>2+</sup>	Cu <sup>2+</sup>  Cu	4	332.5	20	60

A plot of the momentary discharge current density *versus* time is shown in Fig. 5. This experiment was carried out in sunlight as well as with a quartz-halogen lamp. While the battery was being charged, the open-circuit potential between the two platinum electrodes was measured at intervals of 10 min (Fig. 6). The dark potential, *i.e.* the potential before charging, was

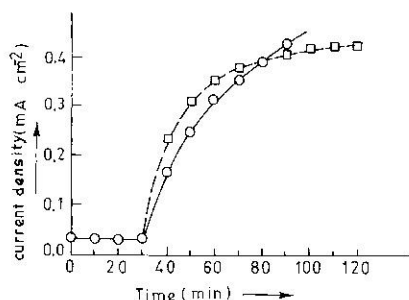


Fig. 5. A plot of current density *vs.* time of charging for the Saur Vidyut Kosh:  $\circ$ , quartz-halogen lamp;  $\square$ , sunlight.

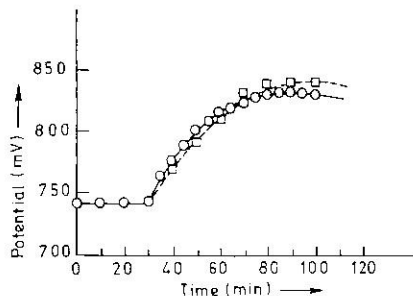


Fig. 6. A plot of potential *vs.* time of charging for the Saur Vidyut Kosh:  $\circ$ , quartz-halogen lamp;  $\square$ , sunlight.

0.74 V and after charging for 60 min it rose to 0.84 V. The potential and current density before charging are due to the difference between the redox potentials of the redox electrolytes present in the two compartments (Figs. 5 and 6). As shown by the horizontal lines in Figs. 5 and 6 the battery was kept short circuited for 30 min before illumination in order to attain equilibrium in the dark. However, the rise in the current between the two platinum electrodes certainly demonstrates the charging process of the cell. The charging and discharging processes were reproducible. The charging efficiency of the cell was calculated as follows:

$$\begin{aligned} \text{charging efficiency} &= \frac{\text{maximum current} \times \text{maximum voltage of the battery}}{\text{maximum photocurrent} \times \text{maximum photovoltage of the photoelectrochemical cell}} \times 100\% \\ &= 72\% \end{aligned}$$

It is because of this high charging rate that the battery almost attains a saturation current within 60 min of the start of charging (Figs. 5 and 6).

### 3. Discussion

In order to obtain the maximum photoresponse, the semiconductor electrode should have a low resistivity and a large space charge region. Hydrogen reduction of  $\text{Pb}_3\text{O}_4$  causes oxygen deficiency, which decreases the resistivity; however, the increase in the donor density decreases the thickness of the space charge region. Since these factors are opposing each other, the best condition is obtained at minimum resistivity and maximum photocurrent. This is why the pellets sintered at  $300^\circ\text{C}$  for 2 h in a hydrogen atmosphere gave the best photoresponse (Table 1). The unexpected increase in

the resistivity of pellets sintered at 350 and 400 °C may be due to the decomposition of  $\text{Pb}_3\text{O}_4$  into  $\text{PbO}$ . This hypothesis is supported by the fact that, when  $\text{Pb}_3\text{O}_4$  is heated in air, decomposition starts at 400 °C [15, 16]. However, in a hydrogen atmosphere, decomposition could start to occur at 350 °C.

Many of the pellets prepared under identical conditions were found not to be reproducible (Section 2.1). This may be because of differences in the densities of the pellets, in the rates of hydrogen reduction and in the critical decomposition temperature of  $\text{Pb}_3\text{O}_4$ . However, the exact cause is not known.

As was shown in Section 2.2.1, the  $\text{Fe}^{3+}|\text{Fe}^{2+}$  redox couple gives a better photoresponse than the  $\text{I}_2|\text{I}^-$  couple because the  $\text{Fe}^{3+}|\text{Fe}^{2+}$  couple produces a larger space charge layer than does  $\text{I}_2|\text{I}^-$  since it has a more positive redox potential. However, the redox couples  $\text{Cr}^{6+}|\text{Cr}^{3+}$  and  $\text{Ce}^{4+}|\text{Ce}^{3+}$  behaved in an unexpected manner because their redox potentials (Fig. 7) fall below the calculated [17] anodic decomposition potential  ${}_pE_d$  of  $\text{Pb}_3\text{O}_4$ . Consequently, the actual oxidation reaction of the electrolyte at the anode is suppressed by the preferred decomposition reaction [17].

According to the Nernst equation,

$$E_{\text{redox}} = E_0 + 0.059 \log \left( \frac{[\text{Fe}^{3+}]}{[\text{Fe}^{2+}]} \right)$$

A comparatively higher ratio of  $[\text{Fe}^{3+}]$  to  $[\text{Fe}^{2+}]$  should give a more positive potential and hence a better photoresponse. This is the trend observed in Table 2 (from a to g). However, a saturated solution of the redox couple should always be used to give faster mass transfer of ions from the bulk of the electrolyte to the electrode surface and faster transfer of charge between the ions and the electrode. A saturated solution of  $\text{Fe}^{3+}$  ions, being dark red, becomes almost opaque to the passage of light. A concentration of  $10^{-1}$  M is therefore used as a compromise for  $\text{Fe}^{3+}$  ions. However, a saturated solution of  $\text{Fe}^{2+}$  ions is not coloured. As a consequence, the combination  $\text{Fe}^{3+}$  (0.1 M)| $\text{Fe}^{2+}$  (saturated) gives the best photoresponse.

It is as a result of slow transfer of mass and charge that the electrode shows some photodecomposition when it is illuminated for 1 h in dilute

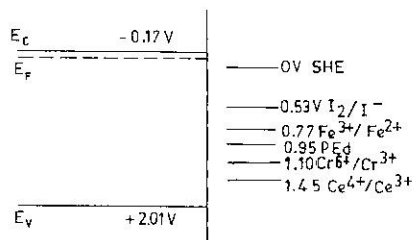


Fig. 7. Energy band diagram of  $\text{Pb}_3\text{O}_4$  based on the experimental results. (The relative positions of the electrolyte redox potentials measured with respect to an SHE are also given.)

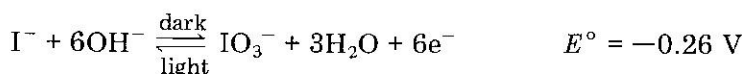
solutions. In this case the oxidation reaction at the anode, although thermodynamically favoured, becomes kinetically unfavourable in competition with the decomposition reaction [17]. However, at higher concentrations such corrosion starts after illumination for 12 h.

The flat-band potential ( $-0.31$  V (SCE)) actually gives the position of the Fermi level of the semiconductor. For a highly doped semiconductor the position of the Fermi level is assumed to be  $0.10$  V below that of the conduction band edge [12]. If we consider our semiconductor to be highly doped, the value of  $E_c$  is given as

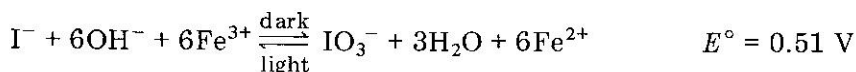
$$\begin{aligned} E_c &= -0.31 - 0.1 \\ &= -0.41 \text{ V (SCE)} \\ &= -0.17 \text{ V (SHE)} \end{aligned}$$

This value of  $E_c$  ( $-0.17$  V) is different from the calculated value (*i.e.*  $0.29$  V (SHE)); this may be because Butler and Ginley [10] made some drastic approximation in calculating the electron affinity of the semiconductor. The energy band diagram based on our experimental results is shown in Fig. 7.

In the Saur Vidyut Kosh the following electrochemical reactions occur:



to give the overall reaction



The potential of the charged battery (*i.e.* of the Saur Vidyut Kosh) should be  $0.51$  V. However, the experimental results suggest that the potential of the charged battery is  $0.84$  V and that the potential of the discharged battery is  $0.74$  V (Fig. 6). This discrepancy is under examination.

#### 4. Conclusion

It was observed that even under identical conditions it is difficult to prepare perfectly reproducible photoanodes from  $\text{Pb}_3\text{O}_4$ . When it is used in a photoelectrochemical cell, this electrode is not photoelectrochemically stable after a period of more than 12 h if the ratio of  $\text{Fe}^{3+}$  ( $10^{-1}$  M) to  $\text{Fe}^{2+}$  (saturated) is maintained. The efficiency of the conversion of solar energy to electrical energy is rather low ( $0.09\%$ ). However, it is possible to make a Saur Vidyut Kosh using  $\text{Pb}_3\text{O}_4$  as the photoanode, provided that the electrode is made more stable. Research is in progress in this direction.



## Acknowledgments

We are grateful to the Council for Scientific and Industrial Research (CSIR) for providing a research grant to carry out this project. One of us (S.K.) is also grateful to the CSIR for providing a fellowship to enable him to carry out this research work.

## References

- 1 A. Fujishima and K. Honda, *Nature (London)*, **238** (1972) 37.
- 2 R. D. Nasby and R. K. Quinn, *Mater. Res. Bull.*, **11** (1965) 985.
- 3 K. L. Hardee and A. J. Bard, *J. Electrochem. Soc.*, **122** (1975) 139.
- 4 K. L. Hardee and A. J. Bard, *J. Electrochem. Soc.*, **124** (1977) 215.
- 5 M. Sharon and A. Sinha, in T. N. Veziroğlu, K. Fueki and T. Ohta (eds.), *Proc. 3rd World Hydrogen Energy Conf., Tokyo, June 23 - 26, 1980*, Vol. 4, Pergamon, Oxford, 1980.
- 6 M. Sharon and A. Sinha, *Int. J. Hydrogen Energy*, **7** (7) (1982) 557.
- 7 J. Manaseen, G. Hodes and D. Lahen, *J. Electrochem. Soc.*, **124** (1977) 532.
- 8 R. Memming, *Philips Tech. Rev.*, **38** (1978) 160.
- 9 F. R. F. Fan, H. White, R. L. Wheeler and A. J. Bard, *J. Am. Chem. Soc.*, **102** (1980) 5142.
- 10 M. A. Butler and D. S. Ginley, *J. Electrochem. Soc.*, **125** (1978) 228.
- 11 M. Sharon and B. M. Prasad, *Sol. Energy Mater.*, **8** (1983) 457.
- 12 D. E. Scaife, *Sol. Energy*, **25** (1980) 41.
- 13 M. A. Butler and D. S. Ginley, *J. Mater. Sci.*, **15** (1980) 1.
- 14 A. V. Pamfilov, *Zh. Fiz. Khim.*, **41** (5) (1967) 1072.
- 15 J. C. Bailar, *Comprehensive Inorganic Chemistry*, Vol. 2, Pergamon, Oxford, 1975, pp. 121 - 122.
- 16 H. Remy, *Treatise on Inorganic Chemistry*, Vol. 1, Elsevier, Amsterdam, 1956, p. 547.
- 17 H. Gerischer, *Top. Appl. Phys.*, **31** (1979) 214.